Probing single-molecule dynamics photon by photon

Haw Yang and X. Sunney Xie

Citation: The Journal of Chemical Physics **117**, 10965 (2002); doi: 10.1063/1.1521154
View online: http://dx.doi.org/10.1063/1.1521154
View Table of Contents: http://scitation.aip.org/content/aip/journal/jcp/117/24?ver=pdfcov
Published by the AIP Publishing

Probing single-molecule dynamics photon by photon

Haw Yang[a] and X. Sunney Xie[b]
Department of Chemistry and Chemical Biology, Harvard University, Cambridge, Massachusetts 02138

(Received 9 April 2002; accepted 18 September 2002)

We present the theoretical rationales for data analysis protocols that afford an efficient extraction of conformational dynamics on a broad range of time scales from single-molecule fluorescence lifetime trajectories. Based on correlation analyses, a photon-by-photon approach on one hand provides the highest time resolution, whereas a minimal-binning method on the other hand is most suitable for experiments experiencing external fluorescence intensity variations. Applications of the two methods are illustrated via computer simulations. In cases where fluorescence quenching is either due to Förster fluorescence resonance energy transfer or due to the excited-state electron transfer, the fluorescence lifetime is dependent on donor-acceptor distance, thereby providing a window through which conformational dynamics are revealed. To assist in interpreting experimental data derived from the new protocols, analytical expressions relating fluorescence lifetime fluctuation correlations to a Brownian diffusion model and to an anomalous diffusion model are discussed.
 [DOI: 10.1063/1.1521154]

I. INTRODUCTION

Single-molecule spectroscopy provides a means by which not only to determine the distribution of molecular properties but also to extract dynamical information that is otherwise concealed in ensemble-averaged experiments.[1] Applications to biophysical studies have been focusing on optically monitoring the working of a single enzyme molecule in real time under ambient conditions.[2] An emerging insight derived from these studies is that a single biological macromolecule is a dynamical entity, the conformation of which may change on a time scale commensurate to or longer than that of a biochemical reaction. As a consequence, its chemical reactivity also fluctuates.[3] In general, the dynamics of conformational changes span many decades of time scales from femtosecond to second. While conformational motions on the submicrosecond time scale have been extensively studied by ensemble-average experiments,[4] the slow and spontaneous conformational fluctuations are difficult to probe because motions of individual molecules are not synchronized on this time scale. The single-molecule approach can optically access time scales ranging from microsecond to minutes. The slow changes in molecular conformations that result in fluctuation in chemical reaction rates have drawn the attention to dynamic disorder.[3,5] Recently, much theoretical work has been put forth in the context of single-molecule studies of dynamical disorder and conformational dynamics,[6–8] which reflects the ever increasing theoretical efforts in the field of single-molecule dynamics since Skinner and co-workers[9] first used stochastic models to interpret low temperature single-molecule spectroscopic data.[10] In this paper, we present the theoretical basis of new methods for studying single-molecule dynamics over the time scales of enzymatic importance.[11]

Optically probing room-temperature structural dynamics at the single molecule level requires monitoring of an experimental observable via the fluorescence of a chromophore. The time evolution of the experimental observable, or trajectory, is analyzed to extract the information on molecular dynamics. The slowest accessible dynamical process, on one hand, is determined by the length of the trajectory—often limited by irreversible photochemical processes that render the fluorophore nonfluorescent. On the other hand, Poissonian statistics (shot noise) of photon detection demand that a number of photons be averaged, or ''binned'' in order to make an accurate measurement of the observable with a certain statistical confidence. It is therefore difficult to observe molecular dynamics that occur on a time scale faster than the binning time.

In this article, we introduce a general methodology that is based on fluctuation-correlation analysis of experimental observables photon by photon. This statistically efficient method not only extends the fast measurable time scale to a microsecond or less, but also allows the education of information from the limited number of detected photons of a single molecule over the time scales that are important in characterizing the function of a biological macromolecule.

We choose fluorescence lifetime as the observable because it is an intrinsic molecular property that reflects the immediate environment of the fluorophore. Examples for single-molecule fluorescence lifetime measurements include tetramethylrhodamine (TMR) dye molecules linked to $tRNA^{Phe}$ and DNA.[12] Those studies showed bi-exponential decay for single-molecule fluorescence, which was attributed to interconversion of conformations of the biomolecule-TMR adducts with the fluorophore being close to and far away from the quencher (guanosine) during the course of the measurements. The new information obtainable from single-

[a]Current address: Department of Chemistry, University of California at Berkeley, Berkeley, CA 94720.
[b]Author to whom correspondence be addressed. Electronic mail: xie@chemistry.harvard.edu

molecule trajectories is the interconversion rates among conformations, which are available neither from the ensemble-averaged nor from single-molecule fluorescence decays. It was proposed that the inter-conversion rates between the two conformational states can be deduced by evaluating the weights of the lifetimes as a function of data acquisition time.[7] In this article, we present a simple and more general approach for directly extracting the interconversion rates using correlation functions.

Consider a macromolecule that has a fluorophore and a quencher that quenches the fluorescence of the former. The fluorescence lifetime of the fluorophore is $\gamma^{-1}=(\gamma_0+\gamma_q)^{-1}$, where γ_0 is the fluorescence decay rate of the fluorophore in the absence of the quencher and γ_q is the quenching rate. Structural fluctuations of the macromolecule may cause changes in the fluorophore–quencher distance, which, in turn, may result in a variation of the quenching rate. In this light, fluorescence lifetime can serve as a sensitive and distance-dependent probe for structural dynamics.

Of particular interest are the cases when the quenching is dominated by a known distance-dependent mechanism. It is then possible to probe directly the fluctuation of fluorophore–quencher distance (x). A widely used mechanism is the FRET quenching,[13] the rate of which can be expressed as $\gamma_q^{\mathrm{FRET}}(t)\cong\gamma_0(R_0/x(t))^6$ if fast randomization for the fluorophore dipole orientation is assumed. x in this case is the center-to-center fluorophore-quencher distance. Here, R_0 is the Förster radius, on the order of 20–80 Å.[14] As a result of the structural fluctuations, the fluorescence lifetime varies in time $\gamma(t)^{-1}=[\gamma_0+\gamma_q^{\mathrm{FRET}}(x(t))]^{-1}$.

In this paper, we discuss the use of the photo-induced ET quenching mechanism as a molecular ruler. The quenching rate γ_q^{ET} in this case depends exponentially on the fluorophore–quencher distance via $\gamma_q^{\mathrm{ET}}(x)=k_0^{\mathrm{ET}}e^{-\beta x}$, where k_0^{ET} is the asymptotic quenching rate, β is a constant characterizing the distance dependence, and x in this case is the edge-to-edge fluorophore–quencher distance. For proteins, k_0^{ET} and β are on the order of 10^{13} s^{-1} and 1.4 $\mathrm{Å}^{-1}$, respectively.[15] The fluorescence lifetime is expressed as $\gamma(t)^{-1}=[\gamma_0+\gamma_q^{\mathrm{ET}}(x(t))]^{-1}$. Here, we seek to directly characterize the interconversion rates between conformational states without resorting to additional statistical analyses,[7] or photon-averaging techniques.[16] We implicitly assume that the time scales of conformational fluctuations are much longer than the fluorescence decay time $\gamma(t)^{-1}$. We consider a molecule that resides in conformational state i at t_i but evolves to conformational state f at some $t_f>t_i$. For a single molecule, such a process is stochastic and can be described by the conditional probability density $H(f,t_f|i,t_i)$. We further assume that the conformational states i and f are characterized by fluorescence lifetimes γ_i^{-1} and γ_f^{-1}, respectively. The time evolution of molecular conformational states can then be characterized by the two-time correlation function of fluorescence lifetime fluctuation of a single molecule,

$$C(t)=\langle\delta\gamma(t)^{-1}\delta\gamma(0)^{-1}\rangle=\langle\gamma(t)^{-1}\gamma(0)^{-1}\rangle-\langle\gamma^{-1}\rangle^2, \quad (1)$$

where $\delta\gamma(t)^{-1}=\gamma(t)^{-1}-\langle\gamma^{-1}\rangle$, and the bracket $\langle\cdots\rangle$ denotes an average over time, which is equal to ensemble averaging under ergodic conditions. For discrete conformational states, the correlation function can be calculated by summing over all states

$$\langle\gamma^{-1}\rangle=\sum_i \gamma_i^{-1}\rho_i,$$

and

$$\langle\gamma(t)^{-1}\gamma(0)^{-1}\rangle=\sum_{f,i}\gamma_f^{-1}H(f,t|i,0)\gamma_i^{-1}\rho_i, \quad (2)$$

where ρ_i is the equilibrium distribution of the ith state.

If there are two discrete states with lifetimes γ_1^{-1} and γ_2^{-1}, and interconversion rates between the two states k_{21} and k_{12}, respectively, it can be shown that $C(t)$ is a monoexponential decay with the decay rate being the sum of k_{21} and k_{12}:[17]

$$C(t)=\frac{(\gamma_1^{-1}-\gamma_2^{-1})^2k_{12}k_{21}}{(k_{12}+k_{21})^2}e^{-(k_{12}+k_{21})t}. \quad (3)$$

This two-state model describes the process of reversible crossing of a barrier separating the two conformational states. $C(t)$ is no longer a monoexponential decay, however, if there are more than two discrete conformational states (or lifetimes) or if there is a continuous distribution of conformational states (or lifetimes).

If the fluorescence lifetime is determined by some continuous dynamic variable such as the fluorophore–quencher distance x, the lifetime correlation is calculated by integrating over the dynamic variable,

$$\langle\gamma^{-1}\rangle=\int\gamma(x)^{-1}dx,$$

and

$$\langle\gamma(t)^{-1}\gamma(0)^{-1}\rangle=\int\int\gamma(x_f)^{-1}H(f,t|i,0)\times\gamma(x_i)^{-1}\rho(x_i)dx_idx_f. \quad (4)$$

Using FRET or ET as spectroscopic rulers for a fluorophore–quencher pair, the lifetime correlation becomes a measure of the projection of multidimensional structural motions to fluctuations in the one-dimensional coordinate specified by the fluorophore–quencher distance.

In practice, $\gamma^{-1}(t)$ is not measured directly in the photon counting detection scheme. Only stochastic realization of $\gamma^{-1}(t)$ is recorded, from which $C(t)$ is calculated. As mentioned earlier, the time scales accessible to single-molecule spectroscopy are limited by the length of the trajectory on the long-time end and by the counting noise in the bin time on the short-time end. The experimental challenge is to develop strategies that allow a faithful characterization of $C(t)$ over a broad range of time scales. This article is intended to provide new data analysis protocols and their theoretical rationales for single-molecule spectroscopy. The new protocols will allow experimentalists in the field to efficiently extract information on fast molecular dynamics. With this in mind, we introduce a photon-by-photon and a minimal-binning approach after briefly reviewing the experimental procedures.

Both methods are based on correlation analyses of the experimental observables—the detected photon delay time. The photon delay time is the realization of the fluorescence lifetime and is stochastic in nature. Conventionally, an averaging (or binning) over many photons is required in order to recover the fluorescence lifetime dynamic variable. In this way, the molecular dynamics that occur on time scales shorter than the bin time are likely to be omitted. Our methods are aimed at circumventing such a shortcoming. The central idea is that one does not need to determine the fluorescence lifetime at every instant of the single-molecule trajectory in order to measure the lifetime fluctuations; the correlation functions can be accurately measured in the presence of uncorrelated stochastic noise. This can be achieved by either analyzing the data photon by photon, or by binning the trajectory with a minimal number of photons per bin.

The photon-by-photon approach involves discretizing the single-molecule trajectory at a time interval such that there is *at most* one photon in each interval. This approach offers the highest time resolution and the most wide-ranging time scales for $C(t)$, and works well in the absence of external intensity modulation such as diffusion or orientational changes. The minimal-binning approach involves binning the single-molecule trajectory with the minimum bin time such that there is *at least* one photon in any time interval. This approach is free from the complications of external intensity moderation that do not arise from molecular structural (lifetime) changes.

These new protocols have led to observations that, in general, $C(t)$ is not monoexponential.[11] The results call for theoretical models that go beyond the simple two-state model. Within the framework of the distance-dependent fluorescence lifetime fluctuations, we discuss two models. The first one is based on Brownian diffusion in a harmonic potential. The second one is based on anomalous diffusion in a harmonic potential describable by the fractional Fokker–Planck equation (FFPE), which has been recently advanced by Klafter and co-workers.[18,19] The FFPE formalism is capable of delineating dynamics that span a broad range of time scales. For these two models, we derive analytical expressions connecting experimentally measurable $C(t)$ and the dynamic variables of each model.

The remainder of the paper is organized as follows: Section II A briefly reviews experimental details for single-molecule fluorescence lifetime measurements. Section II B presents the photon-by-photon approach, whereas Sec. II C presents the minimum bin approach. Simulation and comparison of the various approaches are presented in Sec. II D, where a trajectory of a two-state system is generated by a computer simulation. Section III presents the details of the Brownian and anomalous diffusion models.

II. PROBING MOLECULAR DYNAMICS BY LIFETIME FLUCTUATION CORRELATION

A. Single molecule experiments: Time stamping in time correlated single photon counting (TCSPC)

We begin by briefly reviewing single-molecule fluorescence lifetime measurements.[20] A pico- or femtosecond pulse train is used to excite a single molecule [Fig. 1(a)]. The pulses are typically generated by a passively mode-locked Ti:sapphire laser (76 MHz repetition rate). Once the single molecule is excited, it can recover to the ground state by either emitting a photon (fluorescence), or quenching through FRET or ET or other nonradiative relaxation mechanisms. When the emitted photon is detected by a photodetector such as a single-photon counting avalanche photodiode, the duration between the excitation pulse and the photon-detection event is measured and sorted into a histogram [Fig. 1(b)]. Not every laser pulse excites the molecule, and the count rate of the detected emission photons is typically 1000–200 000 per s. The histogram of the delay times, identical to that of ensemble experiments of TCSPC, gives the survival probability of the excited state. For single dye molecules, the delay time histogram often exhibits a single exponential decay.[20] For single biomolecules, multiexponential decays have been reported.[11] The interconversion rates among the conformers of different lifetimes were not directly measured.

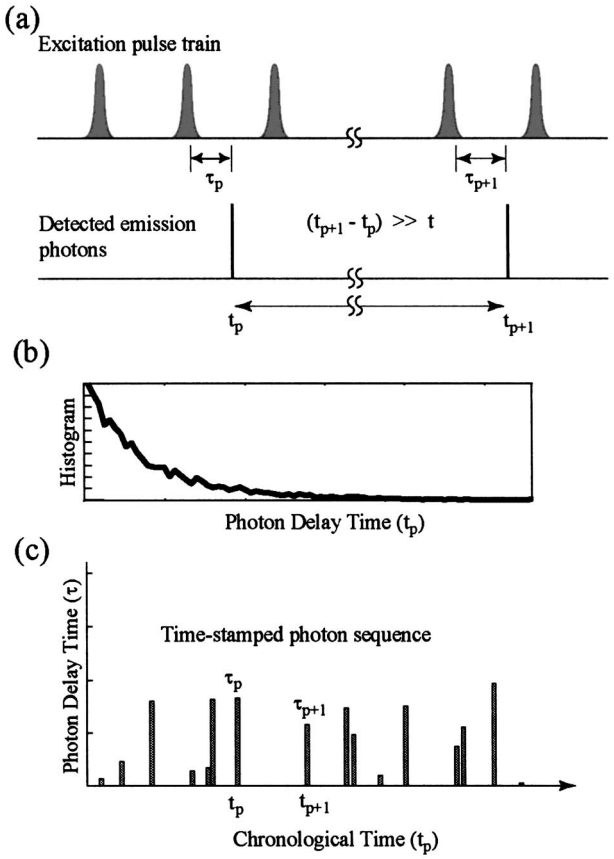

FIG. 1. (a) Schematic representation of a train of excitation pulses and detected emission photons. (b) Histogram of photon delay time τ_p allows for determination of fluorescence lifetime, corresponding to the conventional TCSPC results. (c) Schematic representation of the time-stamped photon sequence. The delay time τ_p and chronological time t_p for each detected photon are sequentially recorded in a computer for data analysis. Note that the two τ and t axes are not on the same scale.

The stochastic delay times of individual photons require that many photons be binned in order to obtain the fluorescence lifetime.[21,22] Therefore, single-molecule lifetime measurements using the binned time-correlation single-photon

counting (TCSPC) data tend to be oblivious to conformational dynamics on a time scale shorter than or comparable to the bin time (as short as ms). Instead of solely building a histogram of the delay time τ of each detected photon relative to its excitation pulse as in the earlier single-molecule lifetime measurements,[20] we record in real time both τ and the chronological time t_p of each detected photon [Fig. 1(c)]. The sequence of such ''time-stamped'' photons, $\{\tau_1(t_1), \ldots, \tau_N(t_N)\}$, is then subjected to statistical analysis. A similar detection scheme has been used by Seidel and co-workers for single-molecule identification and conformational dynamics studies.[16,23] Their data were processed by averaging over every 80 photons, from which the distribution of fluorescence lifetime is constructed and analyzed. It has been recognized that there is more information available should the single-molecule trajectory be analyzed photon by photon. For example, Prummer *et al.*[24] analyze the time- and frequency-stamped detected photon sequence to statistically distinguish four different dye molecules. They show that ~500 photons are needed for a 99% confidence interval certainty for extracting such a *static* distribution. Other methods similar in spirit to the photon-by-photon approach involve analyses of the photon sequence $\{t_p\}$.[25] Those methods are less informative because of the lack of a dynamical variable about which the photons report. Aiming at efficiently extracting *dynamic* information from such a detected photon sequence, we hereby outline two new approaches for studies of conformational dynamics on a single molecule level with a high time resolution and a broad range of time scales.

B. Measuring lifetime correlations in the absence of extrinsic fluorescence intensity variations

1. The approach

It is possible to extract single molecule dynamics utilizing the information carried by each photon. This is applicable in cases where there are no extrinsic fluorescence intensity fluctuations such that changes in the fluorescence lifetime quenching is the only origin of intensity fluctuation, e.g., experiments using immobilized single molecules. Figure 2 shows a simulated experimental recording of the time-stamped photon delay time sequence. The single molecule switches probabilistically between two conformational states, which are distinguishable by their respective intrinsic fluorescence lifetimes $\gamma_1^{-1} < \gamma_2^{-1}$ (indicated by the thick horizontal lines in Fig. 2). The gray vertical lines represent the recorded delay time stamps, which are stochastic observables. Within each conformational state, the lengths of photon delay times are exponentially distributed. Notice that detected photon flux is greater for the more emissive state 2 (longer fluorescence lifetime). To calculate $C(t)$, one may first obtain an accurate estimate of the fluorescence lifetime by averaging over a number of photons (the conventional binning approach), followed by the use of Eq. (1). However, as mentioned earlier, the conventional binning approach tends to be oblivious to dynamics that occur on a time scale shorter than the binning time. On the other hand, if the information carried by each photon can be exploited, a much higher time resolution and hence broader accessible time

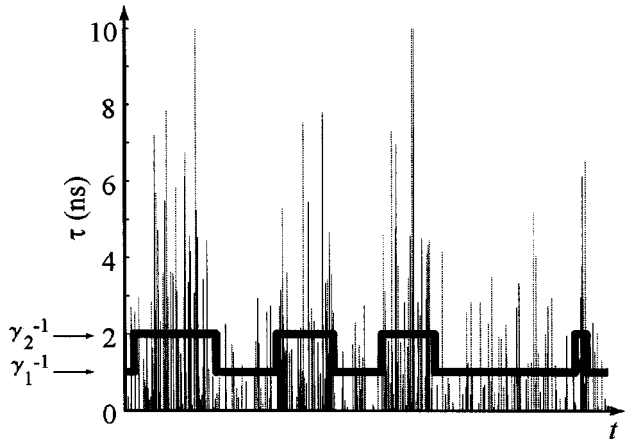

FIG. 2. A simulated experimental trajectory of a single molecule fluctuating between two conformational states with fluorescence lifetimes γ_1^{-1} (1 ns) and γ_2^{-1} (2 ns), assuming the interconversion rates $k_{12}=k_{21}=20\ \mathrm{s}^{-1}$. The trajectory of photon delay times is represented by the gray vertical lines. The trajectory of γ^{-1} is shown by the thick lines. Details of the simulation can be found in Sec. II D.

scale for $C(t)$ can be achieved. In the following, we show that $C(t)$ can be calculated directly from the time-stamped photon sequence $\{\tau_1(t_1), \ldots, \tau_N(t_N)\}$ photon by photon.

2. Photon-by-photon fluorescence lifetime correlation

To extract $C(t)$ from the time-stamped photon sequence $\{\tau_p(t_p)\}$, we consider the fluorescence intensity of a single molecule to be proportional to its excited-state lifetime. We define the ''instantaneous'' fluorescence intensity (or sampling rate) as $I(t)=A_0\gamma(t)^{-1}$. The proportionality constant A_0 is calculated from the mean intensity $\overline{I}$ of the trajectory, and from the mean fluorescence lifetime $\langle\gamma^{-1}\rangle$ by $A_0=\overline{I}/\langle\gamma^{-1}\rangle$. To account for the fact that the expectation value of a dynamic observable is weighed by the sampling rate on a photon-by-photon basis, the lifetime moments are expressed as $(z>-1)$:

$$\langle\gamma^{-z}\rangle=\frac{1}{TA_0}\int_0^T I(t)\,\gamma(t)^{-(z-1)}dt, \tag{5}$$

where T is the trajectory length. We then discretize T into N_s divisions of increment Δ such that $T=N_s\Delta$ and such that there is *at most* one photon in each increment. In an experimental realization that yields the time-stamped photon sequence $\{\tau_p(t_p)\}$, the $I(t_s)$ at time grid t_s can be approximated by $I(t_s)\approx\Sigma_p\hat{u}(t_p-t_s)/\Delta$, where $\hat{u}$ is defined as: $\hat{u}(t_p-t_s)=1$ for $-\frac{1}{2}\Delta\leqslant t_p-t_s<\frac{1}{2}\Delta$ and $\hat{u}(t_p-t_s)=0$ otherwise. With this notation, $\langle\gamma^{-z}\rangle$ becomes, after discretizing the integration,

$$\begin{aligned}\langle\gamma^{-z}\rangle&=\frac{1}{TA_0}\sum_s^{N_s}\gamma(t_s)^{-(z-1)}I(t_s)\Delta\\&=\frac{1}{TA_0}\sum_{s,p}^{N_s}\gamma(t_s)^{-(z-1)}\hat{u}(t_p-t_s)\\&=\frac{1}{TA_0}\sum_p^{N_s}\gamma(t_p)^{-(z-1)}\end{aligned} \tag{6}$$

where t_p marks the chronological time when a photon is detected and the subscript p runs through all detected photons. We next express $\gamma(t_p)$ in Eq. (6) in terms of the experimentally determined stochastic delay time $\{\tau\}$ by sorting the stochastic observable. We note that the sorting procedure only appears in the derivation of the final expressions Eqs. (9) and (10); all sorted photons will be scrambled and reabsorbed in the final sum. An experimentalist does not need to possess *a priori* knowledge as to what category each photon belongs.

We categorize the $\{\gamma(t_p)^{-(z-1)}\}$ terms by the conformational state i from which they arise. Assuming that γ_i^{-1} is the excited state lifetime of the ith conformational state as before, the probability of obtaining a delay time between $\tau - \frac{1}{2}\delta\tau$ and $\tau + \frac{1}{2}\delta\tau$ is $\mathsf{F}_i(\tau)\delta\tau$. The probability density of obtaining a photon delay time stamp of length τ is given by the exponential distribution

$$\mathsf{F}_i(\tau) = \gamma_i \exp(-\gamma_i \tau). \tag{7}$$

The zth lifetime moment for the ith state ($z > -1$; $z \in \Re$) can be expressed as,

$$\gamma_i^{-z} = \int_0^\infty \tau^z \frac{\mathsf{F}_i(\tau)}{\Gamma(1+z)} d\tau \approx \sum_j \tau_j^z \frac{\mathsf{F}_i(\tau)\delta\tau}{\Gamma(1+z)} = \sum_j \tau_j^z \frac{1}{\Gamma(1+z)} \frac{n_{ij}}{\Sigma_j n_{ij}}, \tag{8}$$

where n_{ij} is the number of i-state photons that fall into the jth digitization channel of τ. After sorting p into i the lifetime moments in Eq. (8) becomes

$$\langle \gamma^{-z} \rangle = \frac{1}{TA_0} \sum_i \sum_j \sum_{u=1}^{n_{ij}} \gamma_i (t_{iju})^{-(z-1)} = \frac{1}{TA_0} \sum_p \frac{\tau_p^{z-1}}{\Gamma(z)}, \tag{9}$$

where u is a dummy variable for summation that counts the number of photons in the i state and j digitization channel. Similarly, it can be shown that the correlation function can be expressed by the time-stamped photon sequence as (for $t > 0$ with $z_1, z_2 > -1$ and $z_1, z_2 \in \Re$)

$$\langle \gamma(t)^{-z_1} \gamma(0)^{-z_2} \rangle = \frac{1}{(T-t)A_0^2 \Delta} \sum_{\{q>p\},\{p\}} \frac{\tau_q^{z_1-1}}{\Gamma(z_1)} \times \hat{u}(t_q - t_p - t) \frac{\tau_p^{z_2-1}}{\Gamma(z_2)}. \tag{10}$$

Equations (9) and (11) are our first and second major results, which connect the fluorescence lifetime moments to experimentally realizable yet stochastic quantities $\{\tau_p\}$. Conceptually, the term after the first equal sign in Eq. (9) indicates a sorting of the $\{\tau_p\}$ sequence by conformational states $\{i\}$, and by the digitization channels $\{j\}$.

At this point, the correlation function of lifetime fluctuation in Eq. (11) can be calculated using Eqs. (9) and (11) on a photon-by-photon basis. It should be noted that the uncorrelated background photons do not contribute to the lifetime autocorrelation function. This can be seen by decomposing Eq. (1) into a time-independent and a time-dependent part

$$C(t) = \langle \delta\gamma(t)^{-1} \delta\gamma(0)^{-1} \rangle \equiv \langle \delta\gamma^{-2} \rangle \tilde{C}(t), \tag{11}$$

where $\tilde{C}(t)$ is the time-dependent normalized correlation function, defined as

$$\tilde{C}(t) = \frac{\langle \delta\gamma(t)^{-1} \delta\gamma(0)^{-1} \rangle}{\lim_{t\to 0} \langle \delta\gamma(t)^{-1} \delta\gamma(0)^{-1} \rangle}. \tag{12}$$

In this way, the uncorrelated background photons only add to the time-independent variance $\langle \delta\gamma^{-2} \rangle$ whereas the dynamics are contained in the normalized, time-dependent $\tilde{C}(t)$.

3. Discussion

It merits mentioning some advantages pertaining to our photon-by-photon method. Since every photon counts as a data point, it allows statistically efficient extraction of the dynamic information from a single-molecule trajectory of a limited length. Furthermore, if there are an infinite number of photons, the time resolution of the correlation function is determined by the chronological-time discretization width Δ which is typically limited by the dead time (a few ns to hundreds of ns) of the detection system. This offers the possibility of probing single-molecule conformational fluctuations on the same time scale as that of molecular dynamics simulations.

When $z_1 = z_2 = 1$, the lifetime correlation function of Eq. (11) is identical to the widely used intensity autocorrelation. Such intensity autocorrelation can be experimentally determined with the high time resolution from the time sequence of $\{t_p\}$. Nevertheless, lifetime correlation functions at higher orders [for $z_1 > 1, z_2 > 1$ in Eq. (10)] yield more information than the intensity autocorrelations. In particular, the higher-order terms in Eqs. (9) and (11) are essential for relating the lifetime fluctuation to the fluorophore–quencher distance fluctuation correlation function $C_x(t)$, from which the power spectrum of the distance fluctuation can be calculated by the Wiener–Khintchine theorem. Appendix A gives the recipe for obtaining the power spectra on a photon-by-photon basis.

C. Obtaining dynamic information amid extrinsic fluorescence intensity variations

1. The approach

In the presence of extrinsic fluorescence intensity modulation, the detected photon flux $I(t)$ does not depend solely on the fluorescence lifetime; that is, the expression $I(t) = A_0 \gamma(t)^{-1}$ is no longer valid. Therefore, a proper weighing of the time-trajectory averaging [cf. Eq. (5)] cannot be accomplished. For example, for a single molecule diffusing through an excitation volume, the detected photon flux is moderated by the relative position of the molecule to the focus of the laser beam. Hence, A_0 becomes time dependent. Without the *a priori* knowledge of the dependence of A_0, one resorts to binning of lifetimes in fixed time intervals in order to obtain the properly weighed $C(t)$. The conventional binning approach used long time intervals,[23] which afford lifetime with high accuracy at the expense of time resolution. We use the minimum time interval such that all intervals in a

trajectory contain *at least* one photon. The procedure gives the highest time resolution and broadest time span of $C(t)$ in the presence of external intensity modulations.

It is important to stress that the measurement of lifetime fluctuations with the minimal binning method is more informative and advantageous than intensity correlation measurements [fluorescence correlation spectroscopy (FCS)].[26] FCS-type measurements are complicated by intensity modulations that are not originated from lifetime fluctuations. For example, the intensity correlations will likely contain components resulting from diffusion of a single molecule within the excitation volume of a focused laser beam. On the other hand, since fluorescence lifetime is an intrinsic observable that bears the characteristics of the molecular state, single-molecule lifetime measurements can be, in principle, free from such unwelcome intensity modulations.

We note that, unlike the situation of the photon-by-photon approach, lifetime correlation functions obtained by the minimal binning approach might be contaminated by the existence of significant background photons, which appear to show ''different'' lifetimes. In practice, background counts should be minimized when using the minimum binning approach.

2. Minimal binning fluorescence lifetime correlation

Following the previous discussion, the single-molecule time trajectory is now discretized with some time increment $\Delta_{\max}$ such that there is *at least* one photon in each chronological time increment in the absence of background photons. This procedure constitutes the minimal amount of binning, and hence the name ''minimal binning'' method. The trajectory length in time is $T=N_w\Delta_{\max}$. A convenient choice of $\Delta_{\max}$ is $\Delta_{\max}=\max(\Delta_p)$, where $\Delta_p\equiv t_{p+1}-t_p$ is the difference in the chronological time index between consecutively detected photons. Suppose that, within the interval $\Delta_{\max}$ at time index t_w, n_w photons are detected with delay time stamps $\{\tau(t_p)\}$ where $t_{w-1}\leqslant t_p<t_w$. We introduce an auxiliary random variable $\overline{\tau}(t_w)\equiv\Sigma_{t_{w-1}\leqslant t_p<t_w}\tau(t_p)/n_w$ that serves as a representation of the fluorescence lifetime γ_i^{-1} of state i. The probability density of the new random variable, however, also depends on the number of photons m within a $\Delta_{\max}$ interval and is expressed as a conditional probability $\mathsf{F}_i(\overline{\tau}|m)$. This can be understood as follows: Since $\overline{\tau}$ is the arithmetic mean of m exponentially-distributed τ [cf. Eq. (7)], the functional form of the conditional probability density is given by the gamma distribution

$$\mathsf{F}_i(\overline{\tau}|m)=m\gamma_i\frac{(m\gamma_i\overline{\tau})^{m-1}}{(m-1)!}\exp(-m\gamma_i\overline{\tau}). \tag{13}$$

By ''thought sorting'' through all $\overline{\tau}$ realizations $\{\overline{\tau_w}\}\rightarrow\{\overline{\tau}_{imj}\}$ according to the conformation state i, the number of photons in each interval m, and digitization channel j, we have the zth lifetime moment (a more detailed derivation is included in Appendix B):

$$\langle\gamma^{-z}\rangle\approx\sum_i\sum_m\sum_j\overline{\tau}_j^z b(z,m)\mathsf{F}_i(\overline{\tau}_j|m)\,\delta\overline{\tau}_j P(m|i)P_i$$

$$\approx\frac{1}{N_w}\sum_w\overline{\tau}_w^z b(z,m), \tag{14}$$

where $b(z,m)=m^z\Gamma(m)/\Gamma(m+z)$ is a normalization constant that is applied to every m-photon realization of $\overline{\tau}$. $b(z,m)$ ensures the recovery of γ^{-z} from integration of $\overline{\tau}^z b(z,m)\mathsf{F}(\overline{\tau}|m)$, where the functional form of $\mathsf{F}(\overline{\tau}|m)$ follows Eq. (13). We note that, as expected, Eq. (14) becomes a simple arithmetic mean of $\overline{\tau}$ since $b(1,m)=1$ for all m.

A similar, but more laborious thought-sorting procedure can be applied for calculating the correlation function

$$\langle\gamma(t_w)^{-z_1}\gamma(0)^{-z_2}\rangle\approx\frac{1}{N_w-h}\sum_{u=1}^{N_w-h}b(z_1,m_u)\overline{\tau}^{z_1}(t_u)$$

$$\times b(z_2,m_{u+w})\overline{\tau}^{z_2}(t_u+t_w), \tag{15}$$

where m_u is the number of photons contained in $\overline{\tau}(t_u)$, $b(z,m)$ is a normalization constant as defined before, and $h=t_w/\Delta_{\max}$. Since Eqs. (15) and (16) sample the single-molecule time trajectory on equal time intervals, these two equations are especially advantageous for use in analyzing experimental data that contain unwelcome emission intensity modulations. It ought to be noted that, as in the previously discussed photon-by-photon approach, the minimal-binning approach gains information of $C(t)$ with high time resolution at the expense of the precise knowledge of fluorescence lifetime at every instant of the single-molecule trajectory. The uncorrelated random fluctuations of the auxiliary stochastic observable $\overline{\tau}$ only add to the variance $\langle\overline{\tau}(0)^2\rangle$ and do not contribute to $C(t)$ for $t>0$.

The time resolution of the minimal-binning approach, $\Delta_{\max}$, is found to be dependent of the total number of photons, N, in a single-molecule trajectory via $\Delta_{\max}\propto\log_e N$ (Appendix C). The conventional binning approach requires approximately 100 photons[21] for each lifetime measurement, limiting the time resolution to about $100/\overline{I}$, where $\overline{I}$ is the average detected photon flux of the single-molecule time trajectory. For example, for an average photon detection rate of 50 kHz, the time resolution for such an approach is approximately 2 ms. If the number of detectable photons from a single molecule is approximately 10^5, the statistical time resolution for our ''minimal binning'' scheme is $\sim$230 μs, nearly seven times better than binning every 100 photons.

D. Comparison of different methods by computer simulations

1. A two-state model

We consider the molecular structure changes between two distinct conformations 1 and 2 in the ground electronic state

TABLE I. Parameters for computer simulations of time-stamped single-molecule trajectories for a two-state model.

	k_{12} (s^{-1})	k_{21} (s^{-1})	k_{11*} (s^{-1})	k_{22*} (s^{-1})	$k_{1*1}=k_{2*2}$ (s^{-1})
Set 1	50	50	2.75×10^{8}	2.525×10^{10}	2.5×10^{4}
Set 2	50	50	2.75×10^{8}	2.75×10^{9}	2.5×10^{4}
Set 3	50	50	2.75×10^{8}	5×10^{8}	2.5×10^{4}
Set 4	75	25	2.75×10^{8}	2.75×10^{9}	2.5×10^{4}
Set 5	250	250	2.75×10^{8}	5×10^{8}	5×10^{4}

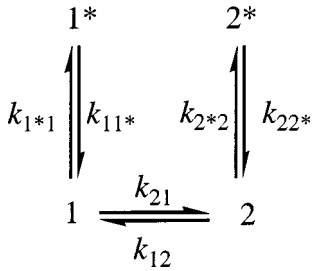

in which k_{12} and k_{21} are the interconversion rates between the two conformers, and k_{11*}^{-1} (or γ_1^{-1}) and k_{22*}^{-1} (or γ_2^{-1}) are the apparent fluorescence lifetimes of states 1 and 2, respectively. The excitation rates k_{1*1} and k_{2*2} were assumed to be equal. For simplicity, we restrict the following discussion to a situation where both k_{12} and k_{21} are time-independent. The correlation function $C(t)$ is given by Eq. (3), which displays a monoexponential decay with the time constant of $(k_{12}+k_{21})^{-1}$ s.

2. Simulation details

We carried out the computer simulations for the two-state single-molecule trajectories following Schenter *et al.*[8] In short, the probability for the molecule to "jump" out of molecular states i during time interval dt was $\Gamma_i dt$, where $\Gamma_i=\Sigma_{f\neq i}k_{fi}$ is the sum of the escape rates and k_{fi} is the kinetic rate of transition from state i to state f. The molecular state could be the ground conformational state 1 (or 2), or its excited states 1* (or 2*). The interconversion time scale $(k_{12}+k_{21})^{-1}$ is assumed to be much greater than that of fluorescence lifetimes γ_1^{-1} or γ_2^{-1}. The fluorescence lifetimes are denoted as k_{11*}^{-1} and k_{22*}^{-1} in the reaction scheme. Five different trajectories were simulated, the parameters of which are listed in Table I. The simulation used a multiple-time step method; the time step for propagating conformational changes was much greater than that for simulating excited state lifetime. The molecule was considered to escape successfully if a random number $y\in[0\ldots1]$ drawn from a uniform distribution was less than $\Gamma_i dt$. Once the molecule had escaped, another random number $z\in[0\ldots1]$ was drawn to determine on which state the molecule would land by comparing z with the probability of reaching state f, k_{fi}/Γ_i. If a transition occurred from a ground conformational state to its excited state, the chronological time t_p is recorded. At this time, the simulation time step was switched from 1 μs per step for conformational propagation to 1 ps per step for excited-state lifetime simulation. If a transition occurred from an excited state to a ground state, the time that the molecule spent in the excited state was recorded as a delay time stamp τ_p, and the (t_p,τ_p) photon stamp was written to a storage device for analysis. This process was repeated until 10^6 photons were collected.

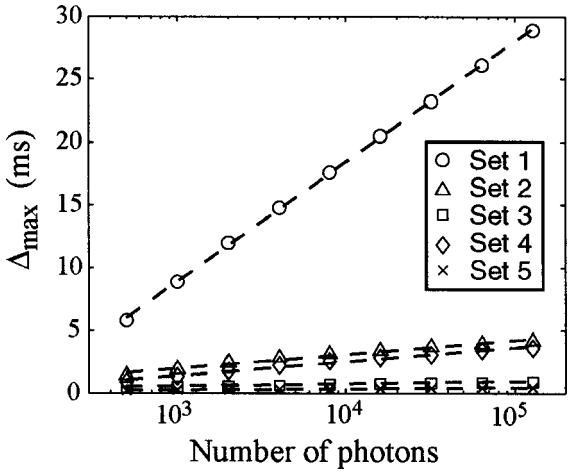

FIG. 3. Plots of the five simulated data sets showing a linear relationship of the minimal bin time Δ_{max} and the logarithm of total of photons, $\log_e N$.

3. The $\Delta_{max}\propto\log_e N$ relation for the minimal-binning procedure

Figure 3 displays plots of Δ_{max} against $\log_e N$ for trajectories containing various numbers of photons. These plots support the results of Appendix C, which argues that for a multiple-state system, the time resolution, Δ_{max}, of a minimally binned single molecule trajectory is determined by the state of the shortest fluorescence lifetime (the least emissive state).

4. Correlation functions

To illustrate the advantage of our new approaches, we simulated a two-state system (set 5) that gives an average fluorescence intensity of 3.57×10^4 photons per second. That is, the conventional 100-photon bin time is ~2.8 ms, longer than the conformational interconversion time (=2 ms). Shown in Fig. 4(a) is a 1500-photon trajectory of the photon delay time τ_p against the chronological time t_p [cf. Fig. 1(c)]. Here, each digitization channel for the photon delay time is set to 3.05 ps. The fluorescence lifetime fluctuation correlation function can be calculated photon by photon using Eqs. (9)–(11). The resulting correlation function is further averaged by binning C(t) with a bin time of $\Delta=1/\overline{I}$ ~0.028 ms to reduce the shot noise, followed by averaging on the log-time scale.[27] The results are shown in Fig. 4(a), which recovers the interconversion time scale $(k_{12}+k_{21})^{-1}$ ~2.1 ms. Shown in Fig. 4(b) is the minimally binned ($\Delta_{max}=0.306$ ms) trajectory of $\overline{\tau}(t_w)$ against t_w containing 164 data points. Despite the reduced time resolution to rectify possible external intensity fluctuation (not assumed in the simulation), the correlation function can still be recovered using Eqs. (14) and (51). The interconversion time [Fig. 4(e), log-averaged] was found to be ca. ~2.3 ms. In contrast, the 1500 photons only give rise to 15 data points if binned

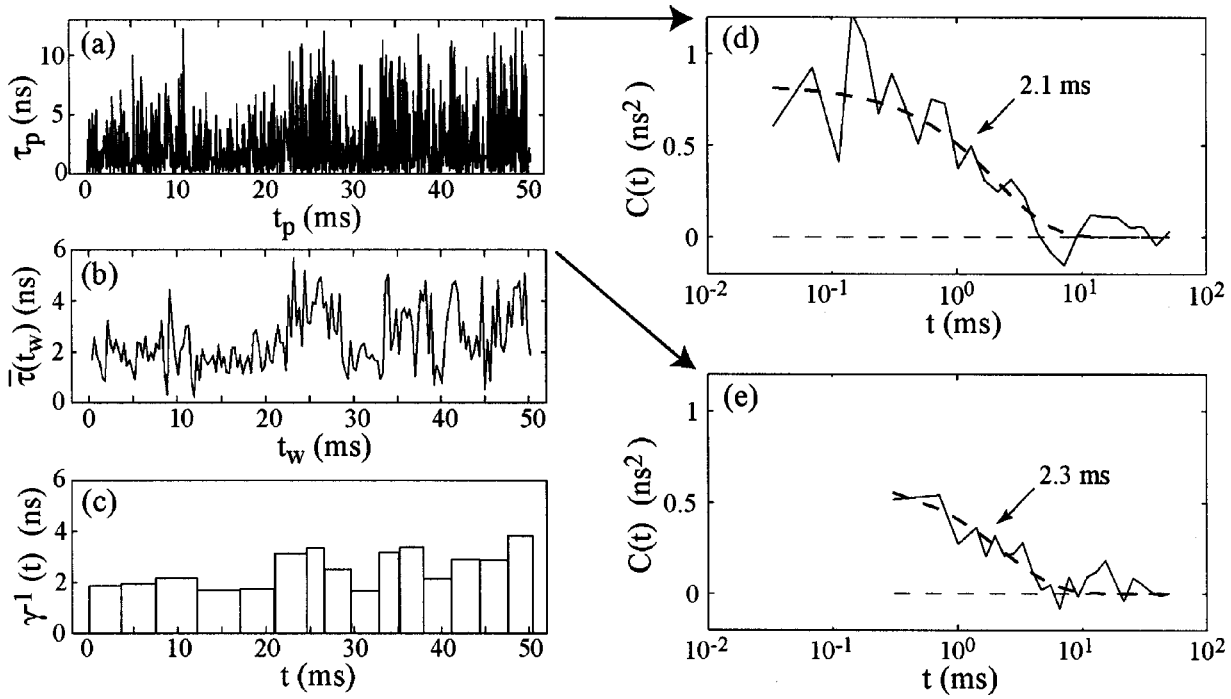

FIG. 4. A computer simulated realization (1500 photons) of a time- stamped single-molecule trajectory of two-state model. The parameters are given in Table I, set 5: (a) The time-stamped delay time $\{\tau(t_p)\}$ trajectory; (b) $\Delta_{\max}$-discretized $\{\bar{\tau}(t_w)\}$ trajectory; (c) 100-photon binned $\{\gamma^{-1}(t)\}$ trajectory; (d) photon-by-photon correlation calculated directory from (a); (e) minimal-binned correlation calculated from (b).

every 100 photons [Fig. 4(c)]; no sensible correlation function can be calculated for such conventionally binned trajectories. These simulations clearly demonstrated the capability of our methods to achieve high time resolution and to probe dynamics that extend over many orders of time scales.

III. FLUORESCENCE LIFETIME CORRELATIONS FOR STRUCTURAL FLUCTUATIONS BEYOND THE TWO-STATE MODEL

We have introduced in Sec. II data analysis protocols for efficiently extracting dynamic information from a single-molecule trajectory. The photon-by-photon and minimal-binning approaches also allow for studies of single-molecule dynamics that cover a wide extent of time scales. New experimental observations have already required theoretical descriptions that are beyond the basic two-state model.[11] We present in the following section formulas that relate the experimentally obtained fluorescence lifetime correlation to two stochastic models, the Brownian diffusion and an anomalous subdiffusion models. Specifically, we derive analytical expressions for fluorescence lifetime quenching dominated by the distance-dependent FRET and ET mechanisms.

A. Brownian diffusion

Consider a situation in which the molecular conformation fluctuations follow the Brownian dynamics. The spatial coordinates for the fluorophore $\mathbf{r}_f(t)$ and the quencher $\mathbf{r}_q(t)$ are stochastic variables [cf. Fig. 5(a)]. The fluorophore–quencher distance displacement $x(t)=|\mathbf{r}_f(t)-\mathbf{r}_q(t)| -\langle|\mathbf{r}_f-\mathbf{r}_q|\rangle$ is also a stochastic variable, the dynamics of which can be modeled as Brownian motion in a harmonic well $V(x)=\frac{1}{2}\mu\omega^2x^2$, where μ is the reduced mass of the fictitious particle [Fig. 5(b)]. In the over-damped limit, the Brownian motion is described by the Langevin equation,[28]

$$\frac{d}{dt}x(t)=-\lambda x(t)+f_x(t), \tag{16}$$

where $\lambda=\omega^2/\eta$ is the drift coefficient that characterizes the correlation time of the stochastic variable $x(t)$ with η being the friction coefficient. The random force exerted on the molecule is contained in $f_x(t)$, which is assumed to be a Gaussian random variable with mean $\langle f_x(t)\rangle=0$ and variance $\langle f_x(t)f_x(t_0)\rangle=2\lambda\theta\delta(t-t_0)$, where $\theta=\langle x^2\rangle=k_BT/\mu\omega^2$ characterizes the magnitude of the fluctuation at room temperatures (fluctuation–dissipation theorem).[5,8] The conditional probability density $H_1(x_1,t_1|x_0,t_0)$ that gives the probability of finding $x(t_1)=x_1$ given $x(t_0)=x_0$, can be solved by standard techniques[29] to give the equilibrium distribution of x

$$\rho_x^{\mathrm{eq}}=\frac{1}{\sqrt{2\pi\theta}}e^{-(x^2/2\theta)} \tag{17}$$

and the fluorophore–quencher displacement correlation,

$$\langle x(t)x(0)\rangle==\theta\, e^{-\lambda t}, \tag{18}$$

which is characterized by only one time scale, the drift time λ^{-1} s.

If the mechanism for the distance-dependent quenching is known, the lifetime correlation can be calculated using Eq. (4) and compared to experimental data. In general, numerical integration will be required for such calculations. However, if the fluorescence lifetime is dominated by the distance-dependent quenching ($\gamma_q\gg\gamma_0$), close-form expressions can

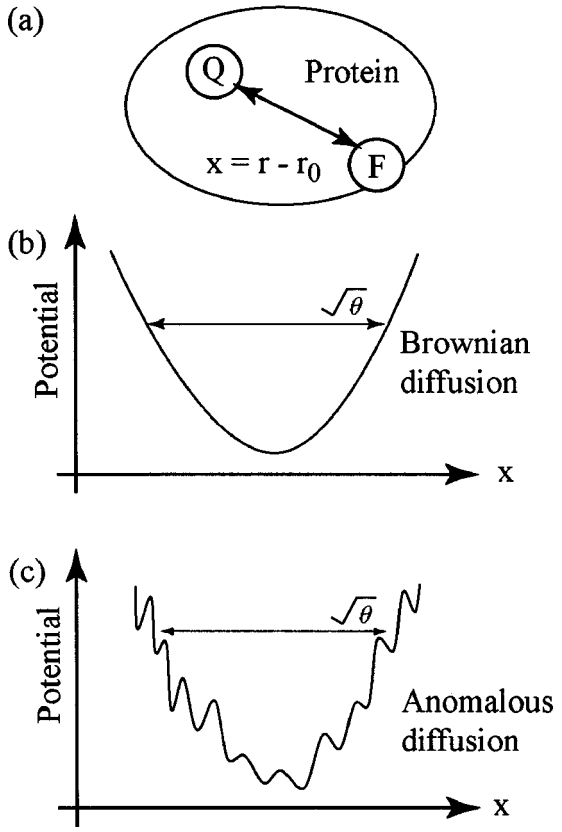

FIG. 5. (a) An illustration showing the use of a fluorophore–quencher pair to probe the conformational dynamics of a single protein molecule. The fluorophore and quencher are denoted F and Q in the figure, respectively. x is the deviation of the fluorophore–quencher distance from its equilibrium value. (b) A sketch representing the relative motions of F and Q as Brownian. The dynamics can be viewed as diffusing along a harmonic potential well. (c) A sketch showing a fictitious particle diffusing along a rugged harmonic potential, representing the subdiffusive behavior.

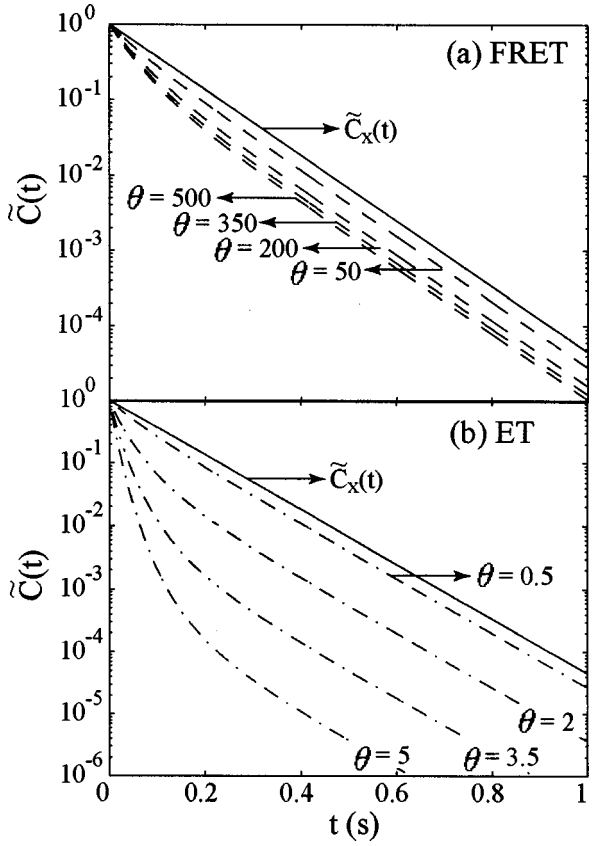

FIG. 6. Plots of Langevin-type conformational dynamics measured by fluorescence lifetime fluctuation correlation via the distance-dependent (a) FRET and (b) ET quenching mechanisms at various θ values. The drift coefficient for the Langevin equation is $\lambda = 10\ s^{-1}$. Other parameters pertinent to the plots are $R_0 = 55$ Å and $x_{eq} = 30$ Å for the FRET mechanism, and $\beta = 1.4\ Å^{-1}$ for the ET mechanism.

be obtained. Here we derive analytical expressions for the FRET and ET quenching mechanisms. In the case of FRET quenching, the fluorescence lifetime is approximated by

$$\gamma^{-1} = [\gamma_0 + \gamma_q^{\mathrm{FRET}}(x)]^{-1} \approx \gamma_q^{\mathrm{FRET}}(x)^{-1} \cong \gamma_0^{-1} R_0^{-6} (x_{\mathrm{eq}} + x)^6, \tag{19}$$

where x_{eq} is the equilibrium fluorophore–quencher distance and x is the fluorophore–quencher displacement as defined before. The lifetime correlation function is then

$$\langle \delta\gamma(t)^{-1} \delta\gamma(0)^{-1} \rangle_{\mathrm{FRET}} = \gamma_0^{-2} \frac{6\theta}{R_0^{12}} \sum_{n=1}^{6} c_n e^{-n\lambda t}, \tag{20}$$

where $c_1 = 6(x_{eq}^5 + 10x_{eq}^3\theta + 15x_{eq}\theta^2)^2$, $c_2 = 75\theta(x_{eq}^4 + 6x_{eq}^2\theta + 3\theta^2)^2$, $c_3 = 400x_{eq}^2\theta^2(x_{eq}^2 + 3\theta)^2$, $c_4 = 900\theta^3(x_{eq}^2 + \theta)^2$, $c_5 = 720x_{eq}^2\theta^4$, and $c_6 = 120\theta^5$. Equation (20) indicates that for molecular structural fluctuations that follow normal diffusive dynamics, the fluorescence lifetime correlation has a well-defined scope of time scales ranging from the short-time cut off $(6\lambda)^{-1}$ s to the long-time cut off λ^{-1} s when reflected through FRET dominated quenching. The long-time cut off can be seen in Fig. 6(a), which shows plots of normalized lifetime fluctuation correlation at different θ values.

Similarly, for ET dominated quenching, the fluorescence lifetime is approximated by

$$\gamma^{-1} = [\gamma_0 + \gamma_q^{\mathrm{ET}}(x)]^{-1} \approx \gamma_q^{\mathrm{ET}}(x)^{-1} \cong [k_0^{\mathrm{ET}} e^{-\beta(x_{\mathrm{eq}} + x)}]^{-1}, \tag{21}$$

which, in turn, gives the lifetime correlation function

$$\langle \delta\gamma(t)^{-1} \delta\gamma(0)^{-1} \rangle_{\mathrm{ET}} = (k_0^{\mathrm{ET}})^{-2} \exp(2\beta x_{\mathrm{eq}} + \beta^2\theta) \times [-1 + \exp(\beta^2\theta e^{-\lambda t})]. \tag{22}$$

At longer times, the lifetime correlation becomes

$$\langle \delta\gamma(t)^{-1} \delta\gamma(0)^{-1} \rangle_{\mathrm{ET}} = (k_0^{\mathrm{ET}})^{-2} \exp(2\beta x_{\mathrm{eq}} + \beta^2\theta) \times \beta^2\theta \exp(-\lambda t). \tag{23}$$

Equations (20)–(23) suggest that the lifetime correlation functions of both FRET- and ET-dominated quenching mechanisms show a long-time cut off on a time scale of $\sim\lambda^{-1}$ s for normal diffusive dynamics, as shown in Fig. 6(b).

In Fig. 6, the short-time curvature of the lifetime correlation functions becomes more prominent as the amplitude of the structural fluctuations becomes greater, as indicated by larger θ values. The fast components, however, can be easily overlooked in measurements with insufficient time resolution. In such measurements, it would be difficult to distinguish a diffusive model from a two-state model since, at long times, both models show only one time constant.

B. Anomalous diffusion in the subdiffusive regime

In the previous model, the Brownian dynamics are characterized by the linear time dependence of mean-square fluorophore–quencher displacement: $\langle x^2\rangle \propto t$ in the force-free limit. For complex systems—including super-cooled liquids, polymers, or biomolecules—deviations from such a linear relationship are often observed.[30] Here we discuss the lifetime correlation when the molecular structural changes follow anomalous diffusion dynamics in the subdiffusion regime in which the mean-square displacement of the fluorophore–quencher distance is characterized by the sublinear power-law dependence: $\langle x^2\rangle \propto t^{\alpha}$, $0<\alpha<1$, again in the force-free limit. This may occur if the trapping time at a particular x has a power-law probability density function $W(t)\propto t^{-(1+\alpha)}$, unlike the situations in the Brownian dynamics where the trapping time has a finite mean. If we assume that the displacement x is bound within a potential, the dynamics can be modeled as a fictitious particle diffusing inside a rugged energy landscape with the potential of mean force $V(x)$ [cf. Fig. 5(c)]. Its dynamics can then be described by the fractional Fokker–Planck equation (FFPE) developed by Klafter and co-workers.[18] Here we use their FFPE solutions to compute the fluorescence lifetime correlation functions. For completeness, we include the definitions of and the solutions to FFPE in Eqs. (24)–(29), the details of which can be found in Refs. 18, 19, and 31. The FFPE has the form

$$\frac{\partial}{\partial t}H_{\alpha}(x,t|x_0,t_0)={}_0D_t^{1-\alpha}\left\{\frac{\partial}{\partial x}\left[\lambda_{\alpha}\frac{dV(x)}{dx}\right]+\lambda_{\alpha}\theta\frac{\partial^2}{\partial x^2}\right\}\times H_{\alpha}(x,t|x_0,t_0), \tag{24}$$

where $\lambda_{\alpha}=\omega^2/\eta_{\alpha}$ is the fractional drift coefficient with the dimension $s^{-\alpha}$ with η_{α} being the generalized friction constant. The Riemann–Liouville fractional operator is defined by

$${}_0D_t^{1-\alpha}H_{\alpha}(x,t)=\frac{1}{\Gamma(\alpha)}\frac{\partial}{\partial t}\int_0^t\frac{H_{\alpha}(x,t')}{(t-t')^{1-\alpha}}dt'. \tag{25}$$

The solution to Eq. (24) is

$$H_{\alpha}(x,t|x_0,t_0=0)=\frac{1}{\sqrt{2\pi\theta}}\sum_{n=0}^{\infty}\frac{1}{2^n n!}E_{\alpha}(-n\tilde{t}^{\alpha})h_n\left(\frac{\tilde{x}_0}{\sqrt{2}}\right)h_n\left(\frac{\tilde{x}}{\sqrt{2}}\right)e^{-\tilde{x}^2/2}, \tag{26}$$

where the reduced parameters are $\tilde{x}=x/\sqrt{\theta}$ and $\tilde{t}=t(\lambda_{\alpha})^{1/\alpha}$. The h_n 's are Hermite polynomials and their eigenvalues here are $\lambda_{n,\alpha}=n\lambda_{\alpha}$. The Mittag–Leffler function is defined through

$$E_{\alpha}(-n\tilde{t}^{\alpha})=\sum_{m=0}^{\infty}\frac{(-n\tilde{t}^{\alpha})^m}{\Gamma(1+m\alpha)}, \tag{27}$$

where $\Gamma(z)=\int_0^{\infty}y^{z-1}e^{-y}dy$ is the gamma function. The Mittag–Leffler function interpolates between an initially stretched-exponential behavior

$$E_{\alpha}(-n\tilde{t}^{\alpha})\approx\exp[-n\lambda_{\alpha}t^{\alpha}/\Gamma(1+\alpha)] \tag{28}$$

and a power-low pattern at long times

$$E_{\alpha}(-n\tilde{t}^{\alpha})\approx[n\lambda_{\alpha}t^{\alpha}\Gamma(1-\alpha)]^{-1}. \tag{29}$$

These approximations lead to analytical expressions for the probability density function $H_{\alpha,S}$ at short-to-intermediate times and $H_{\alpha,L}$ at long times, respectively

$$H_{\alpha,S}(x,t|x_0,t=0)=[2\pi\theta(1-e^{-2\lambda_{\alpha}t^{\alpha}/\Gamma(1+\alpha)})]^{-1/2}\times\exp\left[-\frac{(x-x_0e^{-\lambda_{\alpha}t^{\alpha}/\Gamma(1+\alpha)})^2}{2\theta(1-e^{-2\lambda_{\alpha}t^{\alpha}/\Gamma(1+\alpha)})}\right], \tag{30}$$

$$H_{\alpha,L}(x,t|x_0,t=0)=[2\pi\theta(1-\lambda_{\alpha}^2t^{-2\alpha}/\Gamma(1-\alpha)^2)]^{-1/2}\times\exp\left[-\frac{(x-x_0\lambda_{\alpha}t^{-\alpha}/\Gamma(1-\alpha))^2}{2\theta(1-\lambda_{\alpha}^2t^{-2\alpha}/\Gamma(1-\alpha)^2)}\right]. \tag{31}$$

The fluorophore–quencher displacement correlation functions in these two limiting cases show a stretched-exponential

$$\langle x(t)x(0)\rangle_{\alpha,S}=\theta\,e^{-\lambda_{\alpha}t^{\alpha}/\Gamma(1+\alpha)}, \tag{32}$$

and a power-law behavior

$$\langle x(t)x(0)\rangle_{\alpha,L}=\theta\frac{\lambda_{\alpha}t^{-\alpha}}{\Gamma(1-\alpha)}, \tag{33}$$

respectively.

We next discuss how the subdiffusive dynamics manifest themselves in lifetime correlation via the FRET and ET distance-dependent quenching mechanisms. Generally, the correlation functions are calculated by numerically integrating Eq. (4). However, as in the case of normal diffusion, if the fluorescence lifetime is dominated by the distance-dependent quenching, it is possible to derive analytical expressions for lifetime correlations. Using Eq. (2), we found the lifetime fluctuation correlation at short-to-intermediate time for FRET dominated lifetime quenching to be

$$\langle\delta\gamma(t)^{-1}\delta\gamma(0)^{-1}\rangle_{\mathrm{FRET}}=\gamma_0^{-2}\frac{6\theta}{R_0^{12}}\sum_{n=1}^{6}c_n\exp\left[-\frac{n\lambda_{\alpha}t^{\alpha}}{\Gamma(1+\alpha)}\right], \tag{34}$$

where the c_n 's have been defined previously in the case of normal diffusive model. At long time, the correlation function becomes

$$\langle\delta\gamma(t)^{-1}\delta\gamma(0)^{-1}\rangle_{\mathrm{FRET}}=\gamma_0^{-2}\frac{6\theta}{R_0^{12}}\sum_{n=1}^{6}c_n\frac{\lambda_{\alpha}^nt^{-n\alpha}}{\Gamma(1-\alpha)^n}. \tag{35}$$

Similarly, for ET-quenching dominated lifetime fluctuation [cf. Eq. (22)], we found that the lifetime correlation is

$$\langle\delta\gamma(t)^{-1}\delta\gamma(0)^{-1}\rangle_{\mathrm{ET},S}=(k_0^{\mathrm{ET}})^{-2}e^{2\beta x_{\mathrm{eq}}+\beta^2\theta}[-1+\exp(\beta^2\theta\,e^{-\lambda_{\alpha}t^{\alpha}/\Gamma(1+\alpha)})] \tag{36}$$

on the short-to-intermediate time scale, and

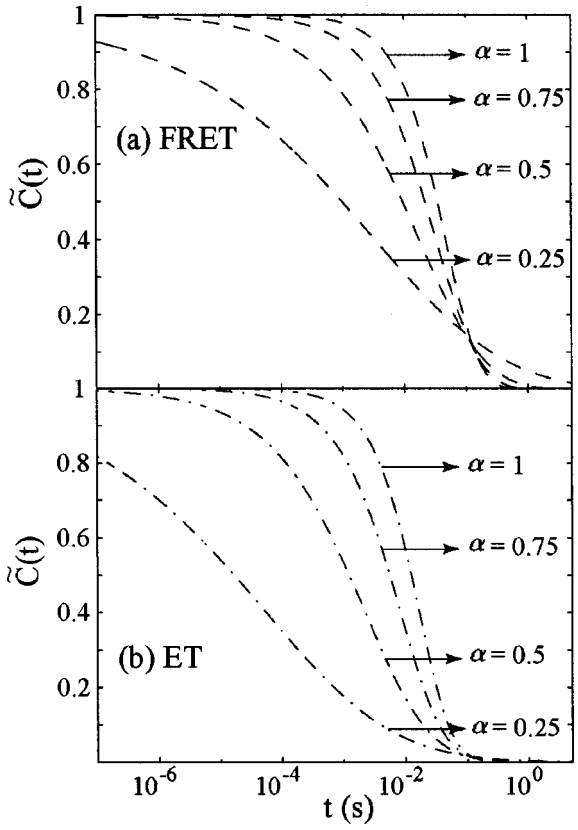

FIG. 7. Plots of conformational dynamics that follow the fractional Fokker–Planck equation and measured by fluorescence lifetime fluctuation correlation via the distance-dependent (a) FRET and (b) ET quenching mechanisms at various α values. The factional drift coefficient λ_α of each plot is adjusted such that the characteristic time scale is the same for all plots; that is, $\lambda_\alpha = (\lambda_c)^\alpha$ in which λ_c is 10 s^{-1}. Other relevant parameters are $R_0 = 55$ Å, $x_{eq} = 30$ Å, and $\theta = 300$ Å^2 for the FRET mechanism, and $\beta = 1.4$ Å^{-1}, and $\theta = 3$ Å^2 for the ET mechanism.

$$\langle \delta\gamma(t)^{-1}\delta\gamma(0)^{-1}\rangle_{\mathrm{ET},L} = (k_0^{\mathrm{ET}})^{-2} e^{2\beta x_{eq}+\beta^2\theta}[-1 + \exp(\beta^2\theta\lambda_\alpha t^{-\alpha}/\Gamma(1-\alpha))] \tag{37}$$

on the long time scale. Eqs. (34)–(37) clearly show that the time scale of the subdiffusive dynamics spans several decades. The lifetime correlations of various α values for the short-to-intermediate time expression are plotted in Figs. 7(a) and 7(b) for FRET [Eq. (34)] and ET [Eq. (36)] quenching, respectively. In both cases, the dynamics stretch across a greater span of time scales as the α value becomes smaller (higher degree of anomaly in diffusion). This is distinctly different from the two-state and the Brownian diffusion model. The dynamics of such a complex system can only be fully understood with experimental strategies that are capable of characterizing single-molecule dynamics on a wide range of time scales. For example, Eq. (36) has been used to describe the conformational dynamics of a single oxidoreductase molecule with an α value of ~0.23.[11]

IV. CONCLUSIONS

In an optical single-molecule experiment, the molecular dynamics are gleaned from the time trajectory of observables such as fluorescence intensity or lifetime. The trajectory is typically constructed by determining the observable value at time t with some statistical certainty. To this end, however, a number of detected photons (~100 typically) are required and the observable value averaged (binned) because of the Poissonian photon statistics. In this article, we outline a new concept for the eduction of molecular dynamics from single-molecule trajectories of finite lengths; the correlation functions of a dynamical variable can be obtained with a high time resolution over a large scope of time scales if binning of the data can be minimized. Such a correlation analysis covers a temporal range that can be two orders broader than the prevailing binning method. As an illustration to this new concept, we choose fluorescence lifetime as the chief observable and discuss its applications.

To implement the idea of utilizing photon statistics to our advantage, we first record a single molecule time trajectory at such a time increment that each time increment contains *at most* one detected photon. In this scenario, the principal time resolution is determined by the instrumentation dead time. In the presence of extrinsic fluorescence intensity alternation that skews the photon-sampling rate, dynamic information can also be obtained efficiently by coarse-graining in time: The single-molecule trajectory is discretized at a time interval Δ_{max} that contains *at least* one detected photon. In this approach, even if 10^5 photons from a single molecule are collected, for instance, our stochastic method offers a time resolution seven times better than the conventional 100-photon binning method. Furthermore, since fluorescence lifetime is an intrinsic molecular property, the extracted dynamics are free from contamination due to time-dependent intensity variations other than those related to the fluorescence lifetime fluctuation.

The new data-analysis protocols may potentially uncover molecular dynamics that are more complicated than the rudimentary two-state morel. To gain further insight from the measured fluorescence lifetime fluctuation correlations, theoretical models that exceed the widely used two-state model will be required. To this end, we derive analytical expressions that relate changes in fluorescence lifetime to the distance-dependent fluorescence resonance energy transfer or excited-state electron transfer quenching for a Brownian diffusion model as well as for an anomalous subdiffusion model. These results corroborate the notion that a methodology that allows characterization of molecular dynamics over several decades of time scales is crucial for a full understanding of a complex system.

We anticipate that this technique will be applicable to single-molecule studies not only of biological but also of nonbiological systems such as glassy polymer melts[32] as well as conducting polymers.[33] The concept of utilizing the information carried by each photon or the sum of a few photons will be equally applicable for other dynamic observables such as emission wavelength.[34] It is expected that the improved time resolution, or expanded observable time scale, will help to better understand complex molecular dynamics by single-molecule experiments.

ACKNOWLEDGEMENT

This work was supported by the National Institutes of Health.

APPENDIX A: OBTAINING POWER SPECTRA VIA MODEL-FREE FLUOROPHORE–QUENCHER DISTANCE CORRELATIONS

If the fluorescence quenching is dominated by a known distance-dependent mechanism, it is possible to probe directly the fluctuation of fluorophore–quencher distance $\langle x(t)x(0)\rangle$ photon by photon. It follows that the temporal behavior of dynamic variables that are related to x can also be obtained. For instance, the power spectrum of molecular structural fluctuation, projected onto the fluorophore–quencher displacement coordinate, can be obtained via the Wiener–Khintchine theorem once $\langle x(t)x(0)\rangle$ is known. In the following, we will give two examples illustrating the mapping between the stochastic delay time τ and the fluorophore–quencher distance x for FRET and ET quenching.

A. FRET

We again assume fast randomization for the fluorophore–dipole orientation. Then, the excited-state lifetime is $\gamma(t)^{-1}=[\gamma_0+\gamma_q^{\mathrm{FRET}}(x(t))]^{-1}$, by which x can be expressed in terms of apparent lifetime $\gamma(t)^{-1}$ as

$$x(t)=R_0(\gamma(t)^{-1}\gamma_0)^{1/6}(1-\gamma(t)^{-1}\gamma_0)^{-1/6}. \tag{A1}$$

The zth moment of x is obtained by first power-series expanding x^z in terms of moments of γ^{-1}, followed by using Eq. (9),

$$\begin{aligned}\langle x^z\rangle &= \sum_{n=0}^{\infty} b_z(n)\left\langle \frac{I(t)}{A_0}\gamma(t)^{-(n+z/6-1)}\right\rangle \\ &\approx \frac{1}{TA_0}\sum_{n=0}^{\infty} b_z(n)\sum_p \frac{\tau_p^{n+z/6-1}}{\Gamma(n+z/6)} \\ &= \frac{R_0^z\gamma_0^{z/6}}{TA_0\Gamma(z/6)}\sum_p \tau_p^{(z/6-1)}e^{\tau_p\gamma_0},\end{aligned} \tag{A2}$$

where $b_z(n)=R_0^z\gamma_0^{(n+z/6)}\Pi_{m=0}^{n-1}(m+z/6)/n!$ are expansion coefficients. The higher moments for fluorophore–quencher distance correlation are $(t>0)$,

$$\begin{aligned}\langle x(t)^{z_1}x(0)^{z_2}\rangle = &\frac{R_0^{(z_1+z_2)}\gamma_0^{(z_1+z_2)/6}}{\Gamma(z_1/6)\Gamma(z_2/6)(T-t)A_0^2\Delta} \\ &\times\sum_{\{q>p\},\{p\}} \tau_q^{(z_1/6-1)}e^{\tau_q\gamma_0}\hat{u}(t_q-t_p-t) \\ &\times\tau_p^{(z_2/6-1)}e^{\tau_p\gamma_0}.\end{aligned} \tag{A3}$$

Equations (A2) and (A3) allow us to calculate the correlation function of $\delta x(t)=x(t)-\langle x\rangle$ in terms of the time-stamped photon sequence

$$C_x(t)=\langle\delta x(t)\,\delta x(0)\rangle=\langle\delta x^2\rangle\tilde{C}_x(t). \tag{A4}$$

B. ET

For fluorescence quenching by electron transfer, the quenching rate γ_q depends on the fluorophore–quencher distance exponentially via $\gamma_q^{\mathrm{ET}}(x)=k_0^{\mathrm{ET}}e^{-\beta x}$, and the time-dependent fluorophore-quencher distance becomes

$$x(t)=\frac{1}{\beta}\ln[\gamma(t)^{-1}k_0^{ET}]-\frac{1}{\beta}\ln\left[1-\frac{\gamma(t)^{-1}}{\gamma_0^{-1}}\right]. \tag{A5}$$

Mapping the photon-by-photon delay time to the fluorophore–quencher distance can then be achieved by expanding x in terms of powers of $\gamma(t)^{-1}$, which can in turn be expressed by stochastic delay times τ. The first term in Eq. (A5) is then

$$\begin{aligned}&\left\langle\frac{1}{\beta}\ln[\gamma(t)^{-1}k_0^{\mathrm{ET}}]\right\rangle \\ &=\frac{1}{\beta}\ln[k_0^{\mathrm{ET}}\gamma_0^{-1}]+\frac{1}{\beta}\sum_{m=0}^{\infty}\frac{1}{m}(-1)^{m-1}\sum_{n=0}^{m} \\ &\quad\times(-1)^n\frac{\Gamma(1+m)}{\Gamma(1+n)\Gamma(1+m-n)}\frac{\langle(\gamma^{-1})^{m-l}\rangle}{(\gamma_0^{-1})^{m-l}}.\end{aligned} \tag{A6}$$

Using Eq. (9), the second term in Eq. (A6) can be written as

$$\frac{1}{\beta TA_0\gamma_0^{-1}}\sum_p\left\{\sum_{n=1}^{\infty}{}_1F_1(1+n,2,-y_p)+\frac{1}{y_p}(1-e^{-y_p})\right\}, \tag{A7}$$

where $y_p\equiv\tau_p/\gamma_0^{-1}$ and ${}_1F_1(a;b;c)$ is the Kummer confluent hypergeometric function and, in the integral representation, has the form

$${}_1F_1(a;b;c)=\frac{\Gamma(b)}{\Gamma(b-a)\Gamma(a)}\int_0^1 e^{cs}s^{a-1}(1-s)^{b-a-1}ds. \tag{A8}$$

Similarly, the second term in Eq. (A5) becomes

$$\left\langle-\frac{1}{\beta}\ln\left[1-\frac{\gamma(t)^{-1}}{\gamma_0^{-1}}\right]\right\rangle=\frac{1}{\beta TA_0\gamma_0^{-1}}\sum_p\frac{1}{y_p}(e^{y_p}-1). \tag{A9}$$

Combining Eqs. (A6) and (A9), we have a mapping of x from the photon delay time sequence $\{\tau_p\}$, renormalized to $y_p=\tau_p/\gamma_0^{-1}$,

$$\begin{aligned}\langle x\rangle=&\frac{1}{\beta}\ln[k_0^{\mathrm{ET}}\gamma_0^{-1}]+\frac{1}{\beta TA_0\gamma_0^{-1}} \\ &\times\sum_p\left\{\sum_{n=1}^{\infty}{}_1F_1(1+n,2,-y_p)+\frac{1}{y_p}(e^{y_p}-e^{-y_p})\right\}.\end{aligned} \tag{A10}$$

The correlation function of x can also be calculated accordingly.

APPENDIX B: DERIVATION OF THE MINIMAL BINNING APPROACH

To recover γ_i from $\{\bar{\tau}\}$, one integrates over realizations of $\bar{\tau}$ and n_w, by analogy to Eq. (8),

$$\gamma_i^{-1}=\sum_m \left[\int_0^\infty \bar{\tau}\mathsf{F}_i(\bar{\tau}|m)d\bar{\tau}\right]P(m|i)$$

$$\approx\sum_m \left[\sum_j \bar{\tau}_j F_i(\bar{\tau}_j|m)\,\delta\bar{\tau}_j\right]P(m|i), \tag{B1}$$

where $P(m|i)$ is the probability of obtaining m photons within the i state. The last term of Eq. (B1) expresses $\bar{\tau}$ in terms of digitized channels $\bar{\tau}_j$ and approximates the integration with a summation. At this point, we can derive the trajectory-averaged fluorescence lifetime by summing over all i conformational states weighed by their respective population P_is:

$$\langle\gamma^{-1}\rangle\approx\sum_i\sum_m\left[\sum_j \bar{\tau}_j F_i(\bar{\tau}_j|m)\,\delta\bar{\tau}_j\right]P(m|i)P_i. \tag{B2}$$

Conceptually, Eq. (B2) means a sorting (building probability functions) of the $\Delta_{\max}$ binned realizations by conformational states $\{i\}$, by the number of photons m in each $\Delta_{\max}$ interval, and by the digitization channels $\{j\}$. As stated earlier in Sec. II B, the sorting procedure is not carried out explicitly since the sorted $\{\bar{\tau}_{imj}\}$ will be scrambled and redistributed in the final summation.

Continuing the derivation, we express P_i as $T_i/T=(n_i\Delta_{\max})/\Sigma_i(n_i\Delta_{\max})=n_i/\Sigma_i n_i=n_i/N_w$, where T_i is the time the molecule spends in conformational state i and n_i is the number of $\Delta_{\max}$ intervals within T_i. Similarly, we have $P(m|i)=n_{im}/\Sigma_m n_{im}=n_{im}/n_i$, where n_{im} is the number of the i-state intervals that contain m photons. Finally, we write the $\mathsf{F}_i(\bar{\tau}_j|m)\,\delta\bar{\tau}_j$ term as $n_{imj}/\Sigma_j n_{imj}=n_{imj}/n_{im}$, where n_{imj} is the number of the i-state, m-photon intervals that has a realization $\bar{\tau}_j$ in the jth digitization channel. With these expressions and the thought-sorting of all $\bar{\tau}$ realizations $\{\bar{\tau}_w\}\rightarrow\{\bar{\tau}_{imj}\}$, the summations in Eq. (B2) becomes

$$\langle\gamma^{-1}\rangle\approx\sum_i\sum_m\left[\sum_j \bar{\tau}_{imj}\frac{n_{imj}}{n_{im}}\right]\left(\frac{n_{im}}{n_i}\right)\frac{n_i}{N_w}\approx\frac{1}{N_w}\sum_w \bar{\tau}_w. \tag{B3}$$

A similar procedure can be carried out for higher order moments to arrive at Eq. (14). The sorting process can also be understood as building histograms for the various conditional probabilities mentioned in the derivation. The fluorescence lifetime is uniformly sampled in this way throughout the single- molecule time trajectory. The detected photon flux does not explicitly enter the expression, thereby removing potential artifacts from global intensity modulations.

We next turn to calculations of the correlation function. As the $\{\bar{\tau}\}$ are sorted by three-label indices, the $\{\bar{\tau}(t_w)\bar{\tau}(0)\}$ product pairs will be classified by six-label indices categorizing the conformational states (f and i), the number of photons in the discretization interval (m_f and m_i), and the delay time digitization channels (j_f and j_i) for $\bar{\tau}(t_w)$ and $\bar{\tau}(0)$, respectively. We start by replacing the γ_i^{-1} and γ_f^{-1} in the correlation function of Eq. (2) with expressions in Eq. (B1),

$$\langle\gamma^{-1}(t_w)\gamma^{-1}(0)\rangle$$

$$\approx\sum_{f,i}\sum_{m_f,m_i}\sum_{j_f,j_i}\bar{\tau}_{f,m_f,j_f}\bar{\tau}_{i,m_i,j_i}P(\bar{\tau}_{j_f}|m_f,f)P(m_f|f)$$

$$\times H(f,t_w|i,0)P(\bar{\tau}_{j_i}|m_i,i)P(m_i|i)P_i,$$

where $P(\bar{\tau}_{j_i}|m_i,i)=\mathsf{F}_i(\bar{\tau}_{j_i}|m_i)\,\delta\bar{\tau}_{j_i}$, and $P(\bar{\tau}_{j_f}|m_f,f)=\mathsf{F}_f(\bar{\tau}_{j_f}|m_f)\,\delta\bar{\tau}_{j_f}$. By Bayes' rule, the above equation can be written as

$$\langle\gamma^{-1}(t_w)\gamma^{-1}(0)\rangle\approx\sum_{f,i}\sum_{m_f,m_i}\sum_{j_f,j_i}\bar{\tau}_{f,m_f,j_f}\bar{\tau}_{i,m_i,j_i}$$

$$\times P(t_w;\bar{\tau}_{j_f},m_f,f,\bar{\tau}_{j_i},m_i,i),$$

where $P(t_w;\bar{\tau}_{j_f},m_f,f,\bar{\tau}_{j_i},m_i,i)$ is the joint probability for obtaining a $\bar{\tau}$ of (i,m_i,j_i) and t_w later, obtaining a $\bar{\tau}$ of (f,m_f,j_f). In the same sprit of building the histogram in arriving at Eq. (B3), we shall now count the members of the six-label indexed $\bar{\tau}$-pair set in the above equation to reconstruct the joint probabilities. Let n_{f,m_f,j_f,i,m_i,j_i} denotes the number of $(\bar{\tau}_{f,m_f,j_f}\bar{\tau}_{i,m_i,j_i})$ pairs, then the said joint probability is

$$P(t_w;\bar{\tau}_{j_f},m_f,f,\bar{\tau}_{j_i},m_i,i)=n_{f,m_f,j_f,i,m_i,j_i}/(N_w-h).$$

The correlation function then becomes:

$$\langle\gamma(t_w)^{-1}\gamma(0)^{-1}\rangle\approx\sum_{f,i}\sum_{m_f,m_i}\sum_{j_f,j_i}\bar{\tau}_{f,m_f,j_f}\bar{\tau}_{i,m_i,j_i}$$

$$\times\frac{n_{f,m_f,j_f,i,m_i,j_i}}{N_w-h}.$$

Expanding the summation and using u to index the $\Delta_{\max}$-discretized single-molecular trajectory, we have the final expression for correlation function:

$$\langle\gamma(t_w)^{-1}\gamma(0)^{-1}\rangle\approx\frac{1}{N_w-h}\sum_{u=1}^{N_w-h}\bar{\tau}(t_u)\bar{\tau}(t_u+t_w). \tag{B4}$$

Equation (B4) again links the fluorescence lifetime correlation to the experimentally measurable, nevertheless stochastic quantities. It has the same form as one would expect for correlation functions of experimental observables. Eq. (B4) can be extended to calculate correlation functions of higher order to give Eq. (15).

APPENDIX C: DEPENDENCE OF TIME RESOLUTION OF THE MINIMAL-BINNING METHOD ON THE SINGLE-MOLECULE TRAJECTORY LENGTH

The time resolution of the correlation function is determined by the width of the discretization interval of the chronological time. In the conventional method using long bin-time intervals of many photons, the time resolution is independent of the trajectory length. In the minimal binning

approach outlined above, however, the time resolution $\Delta_{\max}=\max(\Delta_p)$ depends on the total number of photons in the single-molecule trajectory.

For clarity, we only discuss in detail the case in which there is only one state with fluorescence lifetime γ^{-1} and average detected photon flux $\overline{I}$. In the case of multiple states, the $\Delta_{\max}$ distribution will be determined predominantly by the conformational state that exhibits the lowest emission intensity. For the one-state case, the probability density for obtaining an interphoton duration Δ is $f(\Delta)=\overline{I}\exp(-\Delta\overline{I})$. The corresponding distribution function for interphoton duration shorter than Δ is then, following Ref. 35,

$$\Phi(\Delta)=\Pr(\Delta'\leqslant\Delta)=\int_0^{\Delta}f(\Delta')d\Delta'=1-\exp(-\Delta\overline{I}). \tag{C1}$$

A stream of $N+1$ detected photons with inter-photon durations $\{\Delta_1,\Delta_2,\ldots,\Delta_N\}$ has a maximum $\Delta_{\max}=\max\{\Delta_1,\Delta_2,\ldots,\Delta_N\}$, where the stochastic variable $\Delta_{\max}$ has the distribution function

$$\begin{aligned}\Pr(\Delta_{\max}\leqslant\Delta)&=\Pr(\Delta_1\leqslant\Delta,\Delta_2\leqslant\Delta,\ldots,\Delta_N\leqslant\Delta)\\&=\Pr(\Delta_1\leqslant\Delta)\cdots\Pr(\Delta_N\leqslant\Delta)=\Phi^N(\Delta).\end{aligned} \tag{C2}$$

The renormalized random variable $v\equiv a_N\Delta_{\max}-b_N$ has a limiting distribution function as $N\to\infty$ for $a_N=\overline{I}$ and $b_N=\log_e N$:

$$\begin{aligned}G(v)&=\lim_{N\to\infty}(1-\exp[-(v+\log_e N)])^N\\&\to\exp[-\exp(-v)].\end{aligned} \tag{C3}$$

Equation (C3) is known as Gumbel distribution and has been used to characterize many classes of extreme value problems.[35] We use this limiting distribution to find the expectation value of $\Delta_{\max}$. The expectation value of v for Gumbel density function is

$$E[v]=\int_{-\infty}^{\infty}v\frac{\partial G(v)}{\partial v}dv=\Gamma_{\varepsilon}, \tag{C4}$$

where Γ_{ε} is Euler's constant, defined by $\Gamma_{\varepsilon}=\lim_{N\to\infty}[\Sigma_{m=1}^{N}(1/m)-\log_e N]$ and has a numeric value of $\sim$0.577 216. Using this result, we find that given a stream of $N+1$ detected photons, the expectation value of $\Delta_{\max}$ is

$$E[\Delta_{\max}]_N\approx\frac{1}{\overline{I}}(\Gamma_{\varepsilon}+\log_e N)\approx\frac{1}{\overline{I}}\log_e N. \tag{C5}$$

Statistically, the time resolution for discretizing the single-molecule time trajectory by *at least one photon in each increment* is proportional to the logarithm of the number of detected photons. Eq. (C5) implies that a large $\Delta_{\max}$ (low time resolution) will occur at large N. In practice, any experimentally realizable N ($\sim10^7$ photons) would always result in a better time resolution than the conventional binning method. Therefore, our approach provides a higher time resolution in measuring the correlation functions of single-molecules.

[1] S. M. Nie and R. N. Zare, Annu. Rev. Neurosci. **26**, 567 (1997); X. S. Xie and J. K. Trautman, Annu. Rev. Phys. Chem. **49**, 441 (1998); S. Weiss, Nat. Struct. Biol. **7**, 724 (2000); P. Tamarat, A. Maali, B. Lounis, and M. Orrit, J. Phys. Chem. A **104**, 1 (2000); W. E. Moerner, J. Phys. Chem. B **106**, 910 (2002).

[2] R. D. Vale, T. Funatsu, D. W. Pierce, L. Romberg, Y. Harada, and T. Yanagida, Nature (London) **380**, 451 (1996); H. Noji, R. Yasuda, M. Yoshida, and K. Kinosita, Nature (London) **386**, 299 (1997); R. Yasuda, H. Noji, K. Kinosita, and M. Yoshida, Cell **93**, 1117 (1998); H. P. Lu, L.-Y. Xun, and X. S. Xie, Science **282**, 1877 (1998); L. Edman, Z. Foldes-Papp, S. Wennmalm, and R. Rigler, Chem. Phys. **247**, 11 (1999); X. W. Zhuang, L. E. Bartley, H. P. Babcock, R. Russell, T. J. Ha, D. Herschlag, and S. Chu, Science **288**, 2048 (2000).

[3] X. S. Xie and H. P. Lu, J. Biol. Chem. **274**, 15967 (1999).

[4] G. R. Fleming, *Chemical Applications of Ultrafast Spectroscopy* (Oxford University Press, New York, 1986).

[5] R. Zwanzig, Acc. Chem. Res. **23**, 148 (1990).

[6] J. Wang and P. Wolynes, Phys. Rev. Lett. **74**, 4317 (1995); E. Geva and J. L. Skinner, J. Phys. Chem. B **101**, 8920 (1997); E. Geva and J. L. Skinner, Chem. Phys. Lett. **287**, 125 (1998); A. M. Berezhkovskii, A. Szabo, and G. H. Weiss, J. Chem. Phys. **110**, 9145 (1999); J. N. Onuchic, J. Wang, and P. G. Wolynes, Chem. Phys. **247**, 175 (1999); J. J. Portman and P. G. Wolynes, J. Phys. Chem. A **103**, 10602 (1999); J. Wang and P. Wolynes, J. Chem. Phys. **110**, 4812 (1999); V. Chernyak, M. Schulz, and S. Mukamel, J. Chem. Phys. **111**, 7416 (1999); N. Agmon, J. Phys. Chem. B **104**, 7930 (2000); A. M. Berezhkovskii, A. Szabo, and G. H. Weiss, J. Phys. Chem. B **104**, 3776 (2000); J. S. Cao, Chem. Phys. Lett. **327**, 38 (2000); A. M. Berezhkovskii, M. Boguna, and G. H. Weiss, Chem. Phys. Lett. **336**, 321 (2001); S. L. Yang and J. S. Cao, J. Phys. Chem. B **105**, 6536 (2001); V. Barsegov, V. Chernyak, and S. Mukamel, J. Chem. Phys. **116**, 4240 (2002).

[7] E. Geva and J. L. Skinner, Chem. Phys. Lett. **288**, 225 (1998).

[8] G. K. Schenter, H. P. Lu, and X. S. Xie, J. Phys. Chem. A **103**, 10477 (1999).

[9] P. D. Reilly and J. L. Skinner, Phys. Rev. Lett. **71**, 4257 (1993); P. D. Reilly and J. L. Skinner, J. Lumin. **60–61**, 445 (1994).

[10] W. P. Ambrose, T. Basche, and W. E. Moerner, J. Chem. Phys. **95**, 7150 (1991); M. Orrit and J. Bernard, Phys. Rev. Lett. **65**, 2716 (1990).

[11] H. Yang, G. Luo, P. Karnchanaphanurach, T. Louie, L. Xun, and X. S. Xie (unpublished).

[12] L. Edman, U. Mets, and R. Rigler, Proc. Natl. Acad. Sci. U.S.A. **93**, 6710 (1996); Y.-w. Jia, A. Sytnik, L. Li, S. Vladimirov, B. S. Cooperman, and R. M. Hochstrasser, Proc. Natl. Acad. Sci. U.S.A. **94**, 7932 (1997).

[13] L. Stryer, Annu. Rev. Biochem. **47**, 819 (1978).

[14] B. W. van der Meer, G. Coker III, and S. S. Chen, *Resonance Energy Transfer: Theory and Data* (VCH, New York, 1994).

[15] C. C. Moser, J. M. Keske, K. Warncke, R. S. Farid, and P. L. Dutton, Nature (London) **355**, 796 (1992); H. B. Gray and J. R. Winkler, Annu. Rev. Biochem. **65**, 537 (1996).

[16] C. Eggeling, J. R. Fries, L. Brand, R. Günter, and C. A. M. Seidel, Proc. Natl. Acad. Sci. U.S.A. **95**, 1556 (1998).

[17] H. Yang and X. S. Xie, Chem. Phys. **284**, 423 (2002).

[18] R. Metzler, E. Barkai, and J. Klafter, Phys. Rev. Lett. **82**, 3563 (1999).

[19] R. Metzler and J. Klafter, Phys. Rep., Phys. Lett. **339**, 1 (2000).

[20] S. A. Soper, L. M. Davis, and E. B. Shera, J. Opt. Soc. Am. B **9**, 1761 (1992); X. S. Xie and R. C. Dunn, Science **265**, 361 (1994); W. P. Ambrose, P. M. Goodwin, J. C. Martin, and R. A. Keller, Science **265**, 361 (1994).

[21] M. Köllner and J. Wolfrum, Chem. Phys. Lett. **200**, 199 (1992).

[22] L. Brand, C. Eggeling, C. Zander, K. H. Drexhage, and C. A. M. Seidel, J. Phys. Chem. A **101**, 4313 (1997).

[23] C. Zander, M. Sauer, K. H. Drexhage, D. S. Ko, A. Schulz, J. Wolfrum, L. Brand, C. Eggeling, and C. A. M. Seidel, Appl. Phys. B: Lasers Opt. **63**, 517 (1996).

[24] M. Prummer, C. G. Hubner, B. Sick, B. Hecht, A. Renn, and U. P. Wild, Anal. Chem. **72**, 443 (2000).

[25] A. Molski, J. Hofkens, T. Gensch, N. Boens, and F. De Schryver, Chem. Phys. Lett. **318**, 325 (2000); E. Novikov, J. Hofkens, M. Cotlet, M. Maus, F. C. De Schriver, and N. Boens, Spectrochim. Acta, Part A **57**, 2109 (2001); E. Novikov, N. Boens, and J. Hofkens, Chem. Phys. Lett. **338**, 151 (2001); M. Boguñá, L. Kullman, S. M. Bezrukov, A. M. Berezhkovskii, and G. H. Weiss, J. Phys. Chem. B **105**, 6246 (2001).

[26] D. Magde, W. W. Webb, and E. Elson, Phys. Rev. Lett. **29**, 705 (1972).

[27] K. Schätzel and R. Peters, in *Dynamic Light Scattering: The Method and*

Some Application, edited by W. Brown (Clarendon, Oxford, 1993).
[28] N. G. van Kampen, Stochastic Processes in Physics and Chemistry (Elsevier, Amsterdam, 1992).
[29] H. Risken, The Fokker–Planck Equation, 2nd ed. (Springer, New York, 1989).
[30] J.-P. Bouchaud and A. Georges, Phys. Rep., Phys. Lett. **195**, 12 (1990).
[31] E. Barkai, R. Silbey, and G. Zumofen, J. Chem. Phys. **113**, 5853 (2000); E. Barkai, Y. Jung, and R. Silbey, Phys. Rev. Lett. **87**, 207403 (2001); R. Metzler and J. Klafter, Phys. Rev. E **61**, 6308 (2000); E. Barkai and R. J. Silbey, J. Phys. Chem. B **104**, 3866 (2000).
[32] L. A. Deschenes and D. A. Vanden Bout, Science **292**, 255 (2001); A. P. Bartko, K. Xu, and R. M. Dickson, Phys. Rev. Lett. (to be published).
[33] J. Yu, D. H. Hu, and P. F. Barbara, Science **289**, 1327 (2000).
[34] G. Luo, A. M. van Oijen, H. Yang, E. J. Sanchéz, and X. S. Xie (unpublished).
[35] S. I. Resnick, *Extreme Values, Regular Variation, and Point Processes* (Springer, New York, 1987).